



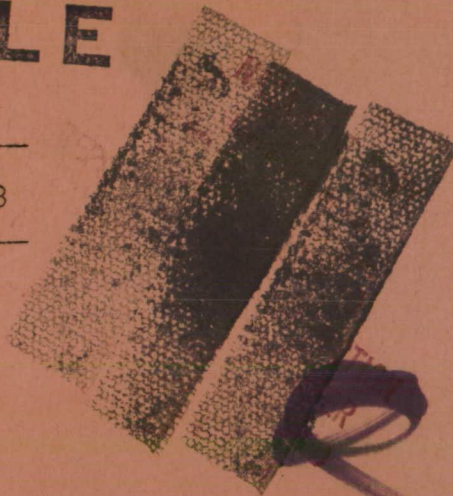
TECHNICAL MEMORANDUMS

C. H. CHATFIELD

NATIONAL ADVISORY COMMITTEE FOR AERONAUTICS.

NACA TM 268CASE FILE
COPY

No. 268

VELOCITY AND PRESSURE DISTRIBUTION BEHIND BODIES
IN AN AIR CURRENT.

By A. Betz.

From Report II, of the Göttingen Aerodynamic Institute.



July, 1924.

NATIONAL ADVISORY COMMITTEE FOR AERONAUTICS.

TECHNICAL MEMORANDUM NO. 268.

VELOCITY AND PRESSURE DISTRIBUTION BEHIND BODIES
IN AN AIR CURRENT.*

By A. Betz.

The following experiments on the air flow behind bodies were made for the purpose of assisting in the explanation of the phenomena connected with air resistance. The resistance or drag of a body is known to be due to two causes. On the one hand, the air flowing along the surface of the body exerts tangentially-directed frictional forces on the body, while on the other hand, the boundary layer behind the body, delayed by the friction, contributes to the formation of the so-called "dead air." Hereby the flow is so changed that the forces normal to the surface of the body have a resultant, which creates a drag. There is manifestly therefore an intimate connection between the flow in the dead air behind a body and the resistance the body experiences. Although no complete explanation of this connection has yet been found, the following experiments may contribute something to that end.

The first two series of experiments dealt with the phenomena behind a cylinder. Here the previously executed drag experiments**

* From Report II, of the Göttingen Aerodynamic Institute, pp.73-77.

** Report II, of the Göttingen Aerodynamic Institute, p.24.

showed that we have to do with two different forms of flow. The one occurs with large and the other with small values of the Reynolds number, the transition taking place at a value vd/ν between 200,000 and 400,000 (v = velocity of wind, d = diameter of cylinder, ν = kinetic viscosity). The experiments were performed with a cylinder of 187 mm (7.36 in.) diameter, first at 35 m (114.8 ft.) per second and then at 15 m (49 ft.) per second. The corresponding Reynolds numbers were $vd/\nu = 45,000$ and $vd/\nu = 200,000$; hence both larger and smaller than the critical. The recording was done in a manner very similar to that employed in the previously described experiments with an unimpeded air-flow. In addition to the dynamic pressure, only the static pressure was plotted, in order to determine not only the energy loss but also how the velocity was affected. The energy loss was given by the difference between the dynamic pressure in the disturbed and undisturbed air-flow, while the velocity v was given by the difference between the dynamic pressure and the static pressure at the point considered, this difference being $\frac{\rho}{2} v^2$, in which ρ = density of air. This distinction was not necessary in the unobstructed air-stream, since there the mean velocity was everywhere nearly parallel to the air-stream, so that the static pressure throughout the whole stream was nearly constant and the dynamic pressure represented both the energy and the velocity. Since the position of the pressure gage corresponded to the direction of the undisturbed air-stream, it was struck somewhat

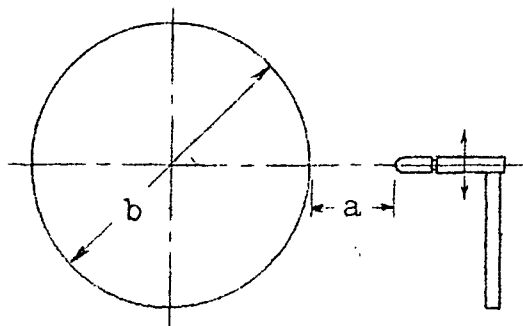
obliquely by the disturbed air behind the cylinder. For a moderate difference in direction (less than 20°) this gave negligible errors. Only at greater angles, did the readings of the gage no longer represent actual conditions.

The pressure gage was placed at various distances a (Fig. 1) behind the cylinder and perpendicular to its axis. The recorded pressures are represented in Figs. 2-11. The straight horizontal line is the zero line. The lines for the dynamic and static pressures are easily distinguished, since the former passes laterally into the dynamic pressure of the undisturbed flow, while the latter approaches the zero line, representing the static pressure of the undisturbed flow. The two vertical lines in each diagram show the diameter of the cylinder. The differences in the curves for the two velocities (Figs. 2-6 on the one hand and Figs. 7-11 on the other) are very evident. At the lower velocity, the negative pressure behind the cylinder is considerably stronger than at the higher velocity, with which the greater drag is also connected. Moreover, the disturbed section is noticeably wider at the lower speed and the flow is much more irregular. This greater irregularity may also be connected with the fact that the adjustment of the velocity differences, or lateral extension of the disturbances, takes place much more rapidly (cf. Figs. 4 and 9).

The third series of experiments was carried out behind a streamlined strut, whose cross-section is shown by Fig. 12. The records were made at a wind velocity of 30 m (98 ft.) per second.

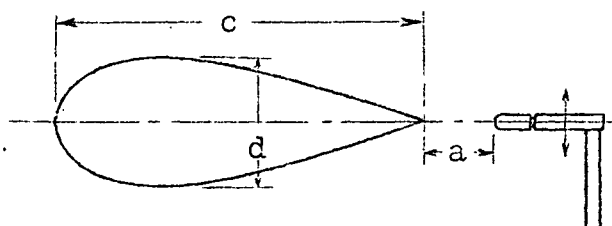
The smallness of the drag of such a strut, $C_D = .05$ (cf. Zeitschrift fu Flugtechnik und Motorluftschiffahrt, 1920, p.54) is clearly shown in Figs. 13-17. Both the width of the disturbed region (The thickness of the strut is indicated by the two vertical lines.) and the magnitude of the disturbance are exceedingly small in comparison with the disturbances behind a cylinder.

Translation by Dwight M. Miner,
National Advisory Committee
for Aeronautics.



$$b=187 \text{ mm}(7.36 \text{ in.})$$

Fig. 1



$$c=250 \text{ mm}(9.84 \text{ in.})$$

$$d= 85 \text{ "}(3.35 \text{ "})$$

Fig. 12

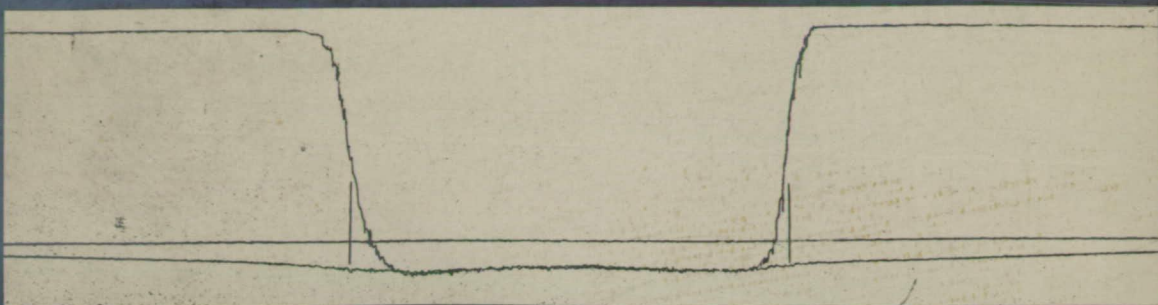


Fig.2 $a = 1 \text{ cm}$ (.394 in.) $q = 76 \text{ kg/m}^2$ (15.57 lb./sq.in.)

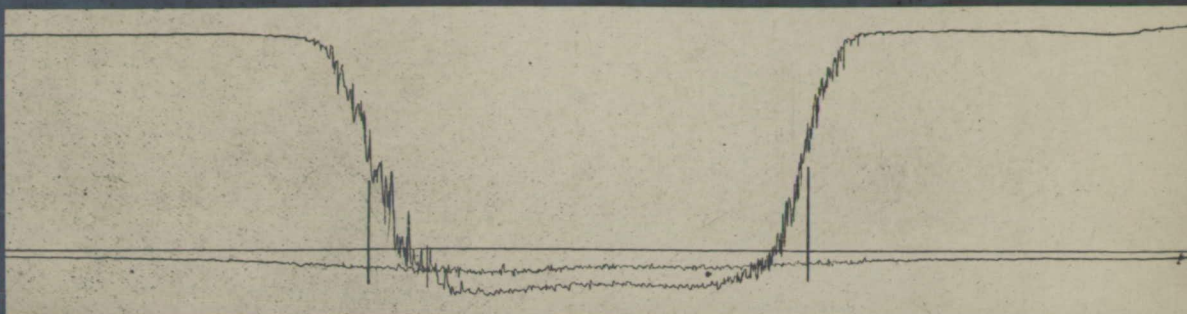


Fig.3 $a = 10 \text{ cm}$ (3.937 in.) $q = 76 \text{ kg/m}^2$ (15.57 lb./sq.ft.)

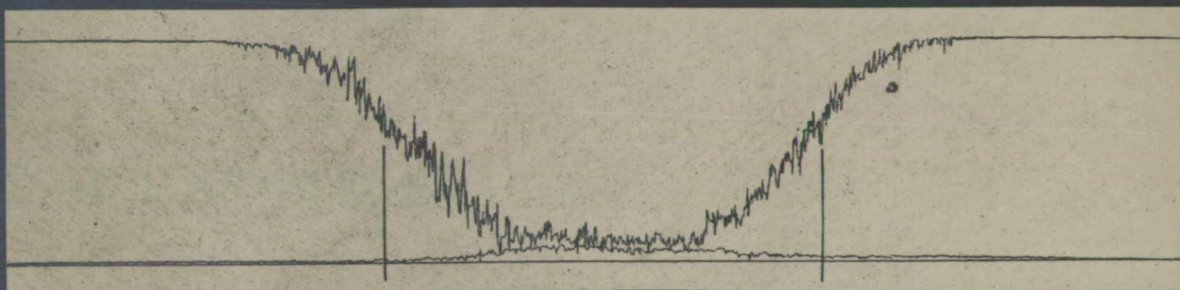


Fig.4 $a = 25 \text{ cm}$ (9.84 in.) $q = 76 \text{ kg/m}^2$ (15.57 lb./sq.ft.)

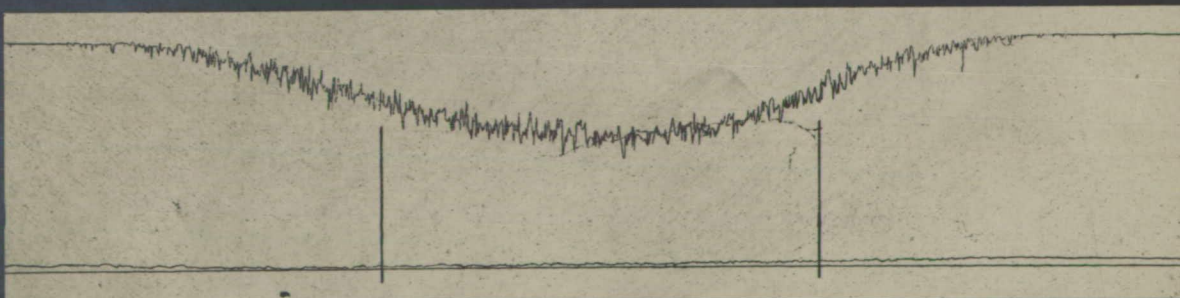


Fig.5 $a = 50 \text{ cm}$ (19.69 in.) $q = 76 \text{ kg/m}^2$ (15.57 lb./sq.ft.)

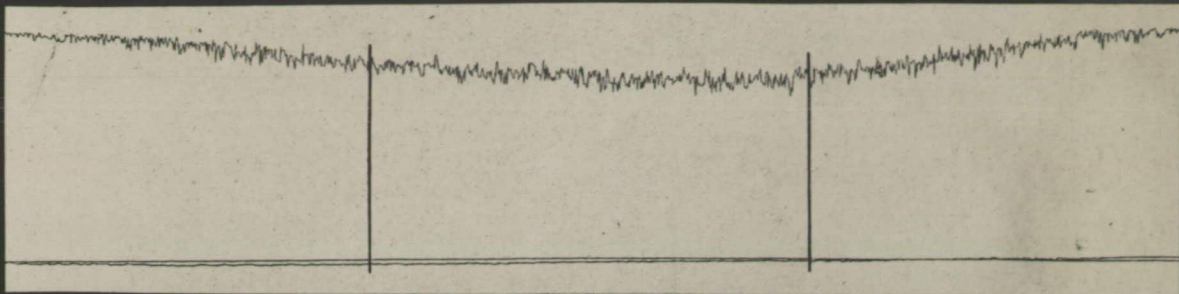


Fig.6 $a = 100 \text{ cm}$ (39.37 in.) $q = 76 \text{ kg/m}^2$ (15.57 lb./sq.ft.)

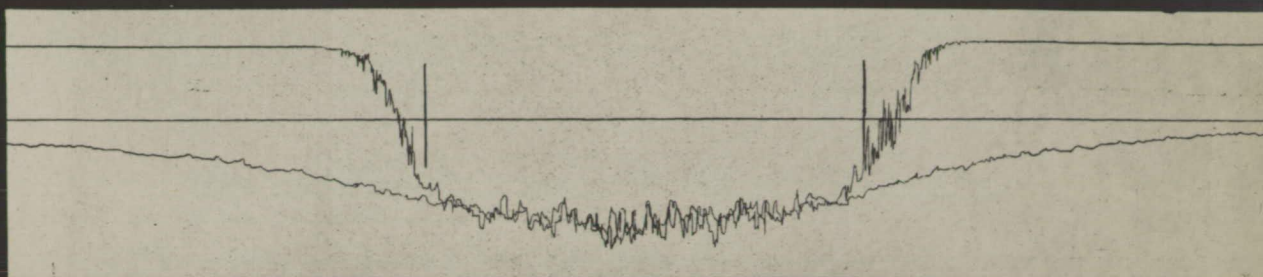


Fig.7 $a = 1 \text{ cm}$ (.394 in.) $q = 14 \text{ kg/m}^2$ (2.87 lb./sq.ft.)

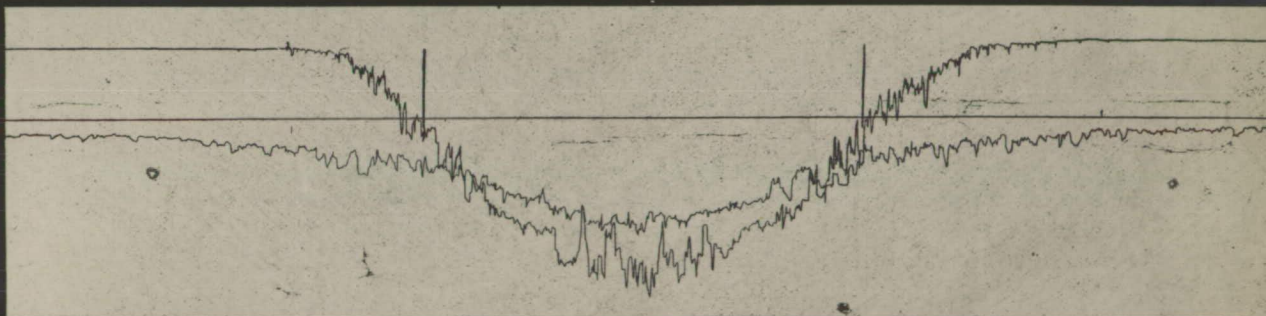


Fig.8 $a = 10 \text{ cm}$ (3.937 in.) $q = 14 \text{ kg/m}^2$ (2.87 lb./sq.ft.)

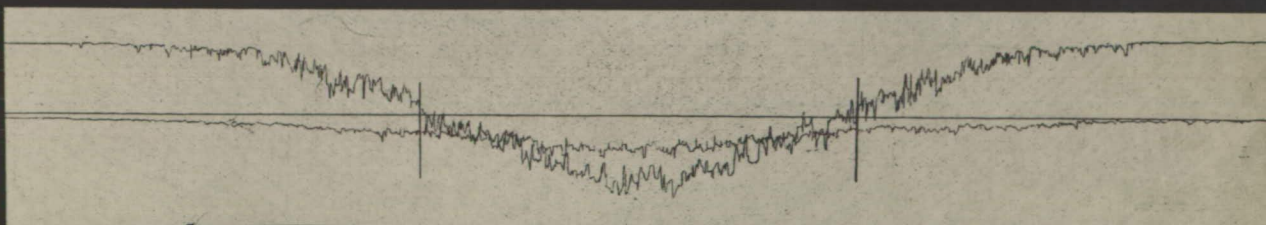


Fig.9 $a = 25 \text{ cm}$ (9.84 in.) $q = 14 \text{ kg/m}^2$ (2.87 lb./sq.ft.)

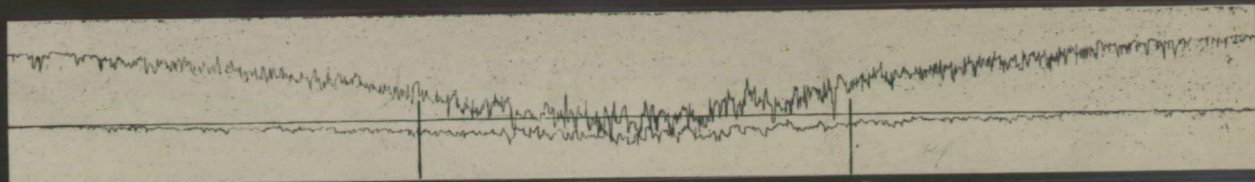


Fig.10 $a = 50 \text{ cm (19.69 in.)}$ $q = 14 \text{ kg/m}^2 (2.87 \text{ lb./sq.ft.})$

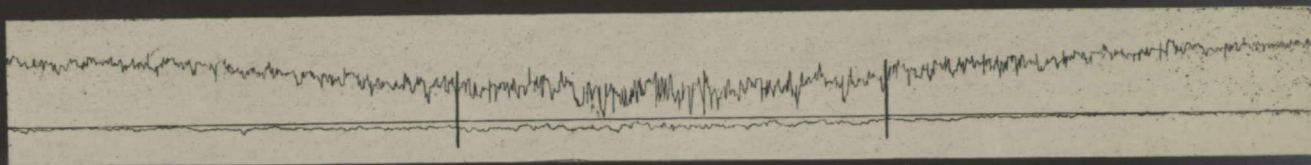


Fig.11 $a = 100 \text{ cm (39.37 in.)}$ $q = 14 \text{ kg/m}^2 (2.87 \text{ lb./sq.ft.})$

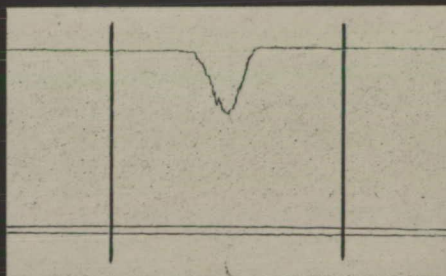
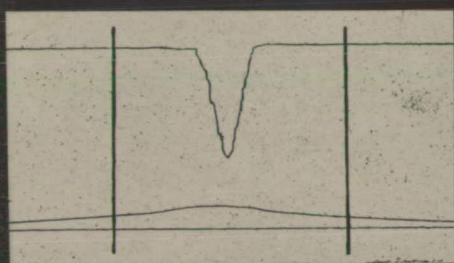


Fig.13 $a = 1 \text{ cm (.394 in.)}$ $q = 56 \text{ kg/m}^2 (11.47 \text{ lb./sq.ft.})$ Fig.14 $a = 10 \text{ cm (3.937 in.)}$ $q = 56 \text{ kg/m}^2 (11.47 \text{ lb./sq.ft.})$

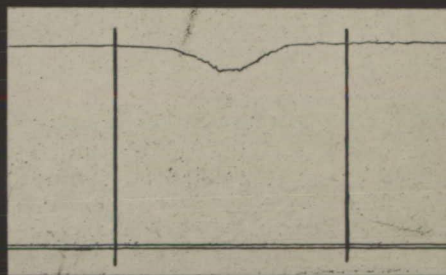
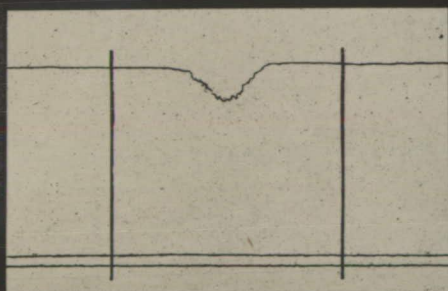


Fig.15 $a = 25 \text{ cm (9.84 in.)}$ $q = 56 \text{ kg/m}^2 (11.47 \text{ lb./sq.ft.})$ Fig.16 $a = 50 \text{ cm (19.69 in.)}$ $q = 56 \text{ kg/m}^2 (11.47 \text{ lb./sq.ft.})$

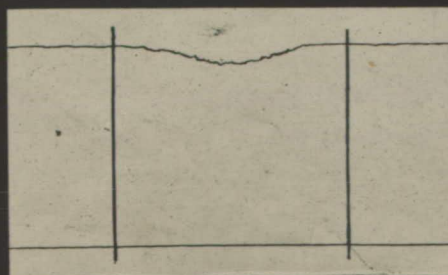


Fig.17 $a = 100 \text{ cm (39.37 in.)}$ $q = 56 \text{ kg/m}^2 (11.47 \text{ lb./sq.ft.})$